Inorganic Chemistry

Communication

pubs.acs.org/IC

New Volatile Strontium and Barium Imidazolate Complexes for the Deposition of Group 2 Metal Oxides

John A. T. Norman,*[,†] Melanie Perez,[†] M. S. Kim,[‡] Xinjian Lei,[†] Sergei Ivanov,[§] Agnes Derecskei-Kovacs,[§] Laura Matz,[§] Iain Buchanan,[∥] and Arnold L. Rheingold[⊥]

[†]Air Products and Chemicals, 1969 Palomar Oaks Way, Carlsbad, California 92011, United States

[‡]R&D Center, Air Products Korea, 15 Nongseo-Dong, Giheung-Gu, Yongin-Si, Gyeonggi-Do 446-920, Korea

[§]Air Products and Chemicals, 7201 Hamilton Boulevard, Allentown, Pennsylvania 18195, United States

[∥]Air Products and Chemicals, Hersham Place, Molesey Road, Walton on Thames, United Kingdom KT12 4RZ

[⊥]Department of Chemistry, University of California at San Diego, La Jolla, California 92093-0358, United States

Supporting Information

ABSTRACT: We report the synthesis, characterization, and experimental density function theory-derived properties of new volatile strontium and barium imidazolate complexes, which under atomic layer deposition conditions using ozone as a reagent can deposit crystalline strontium oxide at 375 °C.

New cleanly volatile strontium and barium precursors are sought for the atomic layer deposition (ALD) of strontium titanate (STO)[1] and barium strontium titanate (BST) dielectrics for the manufacture of advanced dynamic random access memory (DRAM) devices. Developing such precursors is challenging because of the large ionic radii of Sr^{2+} and Ba^{2+} (1.27 and 1.43 Å, respectively), which require bulky and thermally stable ligands to shield and isolate the metal centers from each other to allow low-nuclearity complexes to form.

The most common ligands used to synthesize volatile precursors for strontium and barium are highly substituted β-diketonates such as 2,2,6,6-tetramethylheptanedione[2] and highly substituted cyclopentadienes such as tri-*tert*-butylcyclopentadiene.[3] However, the relatively strong ligand−metal bonds of the β-diketonate precursors coupled with their relatively weak intraligand bonds can lead to low ALD reactivity and high levels of carbon incorporation during metal oxide film growth. In contrast, the cyclopentadienyl precursors have relatively weak ligand−metal bonds but strong intraligand bonds resulting in high ALD reactivity and low levels of carbon incorporation.[4] From this perspective, we selected strontium bis(tri-*tert*-butylcyclopentadienyl), Sr(^{t}Bu$_3$Cp)$_2$, and barium bis(tri-*tert*-butylcyclopentadienyl), Ba(^{t}Bu$_3$Cp)$_2$, as benchmark ALD precursors for STO and BST[5] whose performance we set out to improve upon. We were attracted to how the Sr^{2+} and Ba^{2+} ions are well matched to bulkily substituted five-membered aromatic anions such as ^{t}Bu$_3$Cp that permit η^5 coordination of the ligand to the metals to allow monomer formation. Similarly, the ^{t}Bu groups of 2,5-di-*tert*-butylpyrrolyl flank and protect its nitrogen to permit monomeric η^5 binding to strontium.[6] This led us to contemplate a similar approach using imidazolate, which is isoelectronic with cyclopentandienyl and pyrrolyl, although the η^5 imidazolate coordination mode is exceedingly rare[7] and, aside from theoretical predictions,[8] is unprecedented for Group 2 elements. Multinuclear, dimeric and monomeric Group 2 complexes of isoelectronic five-membered pyrazolate anions substituted in the 3 and 5 positions with *tert*-butyl[9] or phenyl[10] groups have also been reported, including η^5 coordination. However, these compounds tend to be thermally unstable during evaporation.

2,4,5-Tri-*tert*-butylimidazole was synthesized and then reacted with strontium hexamethyldisilazide to yield distrontium tetra(2,4,5-tri-*tert*-butylimidazolate) (**1**) as a volatile colorless crystalline solid (mp 149 °C). Similarly, reaction with barium hexamethyldisilazide yielded dibarium tetra(2,4,5-tri-*tert*-butylimidazolate) (**2**) as a volatile colorless crystalline solid (mp 147 °C). Complexes **1** and **2** were shown to be isostructural by X-ray crystallography. The terminal η^5 imidazolate rings in **2**, shown in Figure 1, are tilted such that

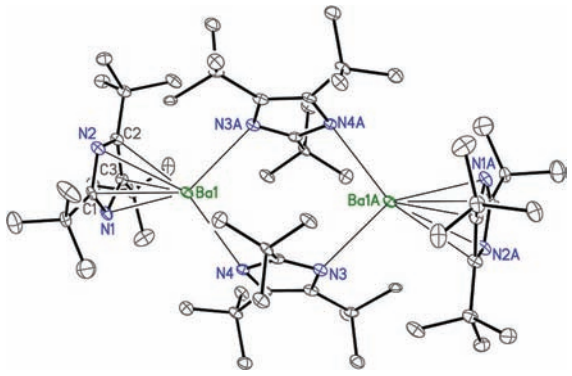

Figure 1. Molecular structure of dibarium tetra(2,4,5-tri-*tert*-butylimidazolate) (**2**).

the three shortest metal−imidazolate bonds are those to C1 [2.831(7) Å], N1 [2.935(6) Å], and N2 [2.939(6) Å]. The longest metal−imidazolate bonds are those to C2 and C3

Received: August 11, 2011
Published: November 21, 2011

[3.110(7) and 3.107(7) Å, respectively]. These differences reflect the concentration of charge density on imdazolate's nitrogens atoms (vide infra) shortening the bonds to C1, N1, and N2. Similarly, the comparable bonds from strontium to C1, N1, and N2 are the shortest in complex **1**. Each of the new imidazolate complexes described herein also contains two μ_2 bridging imidazolates to complete their dimeric structures.

To lower the melting points of **1** and **2**, we introduced imidazole asymmetry by synthesizing 2-*tert*-butyl-4,5-di-*tert*-amylimidazole. Reaction with strontium and barium hexamethyldisilylazide yielded distrontium tetra(2-*tert*-butyl-4,5-di-*tert*-amylimidazolate) (**3**), shown in Figure 2, and dibarium tetra(2-

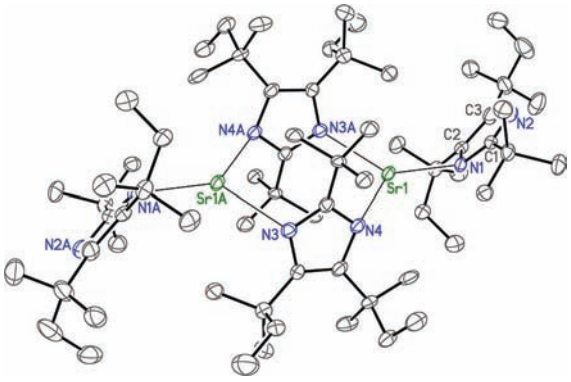

Figure 2. Molecular structure of distrontium tetra(2-*tert*-butyl-4,5-di-*tert*-amylimidazolate) (**3**).

tert-butyl-4,5-di-*tert*-amylimidazolate) (**4**) as volatile colorless solids. The melting points of 103 °C for **3** and 68 °C for **4** represent depressions of 46 and 79 °C, respectively, validating our strategy.

The terminal imidazolates of **3**, shown in Figure 2, are η^1-coordinated, whereas the terminal imidazolates of **4** are η^5, presumably because of the bulk of Ba^{2+} compared to Sr^{2+}. Thermogravimetric analysis (TGA) of these imidazolate complexes showed fewer involatile residues after samples had been heated under a flowing nitrogen atmosphere to 400 °C (**1**, 4.0 wt %; **2**, 3.5 wt %; **3**, 4.0 wt %; **4**, 3.1 wt %) compared to the benchmark cyclopentadienyl precursors [$Sr(^tBu_3Cp)_2$, 10.7 wt %; $Ba(^tBu_3Cp)_2$, 10.3 wt %], the latter two values being consistent with literature results.[3] Because the degree of thermal decomposition of a precursor typically corresponds its amount of involatile residue in the TGA experiment, these results suggest that Sr and Ba imidazolates possess superior thermal stability relative to Sr and Ba cyclopentadienyls bearing similar tertiary alkyl substituents. By TGA techniques,[11] we also measured the vapor pressures of **1**, **3**, and **4** to be ~1 Torr at 170, 210, and 180 °C, respectively. It is notable that the TGA evaporation rates of dimeric complexes **1** and **2** are very similar to those of the known monomers $Sr(^tBu_3Cp)_2$ and $Ba(^tBu_3Cp)_2$,[3] suggesting that the dimeric imidazolates can dissociate to evaporate as monomeric bis(imidazolate) complexes. This was confirmed by GCMS of **1** showing the parent ion of the monomer at 558 mu and the parent ion minus ($^tBu_3$imidazolate) at 323 mu.

To examine the effect of imidazolate substituents on the degree of intermolecular association in Sr imidazolates as a proxy for their volatility, we applied density function theory[12] to calculate dimerization energies (ΔE_{dim}) for strontium dimers containing two η^5 and two μ_2 imidazolates for a range of trisubstituted imidazoles, as shown in Table 1. ΔE_{dim} is defined by eq 1

$$\Delta E_{dim} = E(\text{dimer}) - 2E(\text{monomer}) \quad (1)$$

where E(dimer) and E(monomer) are the total energies of dimers and monomers, respectively, in kilocalories per mole.

Table 1. Energies of Dimerization (E_{dim}) for Strontium Imidazolates with Different Alkyl Substituents in Position 2 and Positions 4 and 5 of Imidazole

position 2	positions 4 and 5	ΔE_{dim} (kcal/mol)
H	H	−48.1
Me	Me	−41.6
^{i}Pr	^{i}Pr	−25
^{t}Bu	^{t}Bu	4.6
^{t}Bu	^{i}Pr	−14.2
^{i}Pr	^{t}Bu	−11.3
^{t}amyl	^{t}Bu	−1.5
^{t}Bu	^{t}amyl	3.4
^{t}Bu	^{s}Bu	−12.4

With small substituents, the formation of dimers is highly exothermic and the energy gained by adding a third or fourth monomer is within ~1 kcal/mol of ΔE_{dim}, ultimately yielding oligomeric nonvolatile structures. Oligomer stability steadily decreases with incrementally larger substituents until, with all tertiary substituents, the formation of dimeric structures becomes almost thermodynamically neutral. Interconversion between the dimer and monomer can occur within approximately ±5 kcal/mol, supporting our observation that dimers can evaporate as monomers.

Electron density mapping of $Sr(^tBu_3Cp)_2$ versus the bis η^5 monomer of complex **1** reveals the latter to possess a greater cationic charge on strontium and negative charge accumulation on its imidazolate nitrogens. This higher degree of ionicity for the imidazolate complex implies higher chemical reactivity, while the electron rich imidazolate nitrogens suggest enhanced surface reactivity toward Lewis acid sites such as OH or metal centers. Additionally, a greater HOMO/LUMO energy gap was calculated for the monomer of **1** (0.2417 eV) than for $Sr(^tBu_3Cp)_2$ (0.2078 eV), supporting the greater thermal stability of the imidazolate complex,[13] experimentally confirmed by our TGA results described above.

Vapors of **3** or **4** pulsed over SiO_2 substrates under ALD conditions from 250 to 450 °C for 50 cycles indicated no significant degradation of **3** or **4** until ~375 or ~350 °C, respectively, as determined by XRF surface density measurements of thermally deposited strontium and barium. Deposition of SrO and BaO films from **3** and **4** was demonstrated using ozone as an oxidant under ALD conditions. Figure 3 shows an approximately ~13 nm thick SrO film grown at 375 °C using 50 cycles of **3**, argon, ozone, and argon onto a SiO_2 substrate and then capped in situ with ~3 nm of TiO_2. Remarkably, the top 6.6 nm layer of SrO is clearly crystalline as deposited. XRD shows a lone $2\theta \cong 50°$ diffraction peak corresponding to the crystalline SrO (220) reflection. XPS shows no nitrogen to be present, indicating the absence of imidazole. The upper surface of SrO shows the presence of carbon, suggesting the formation of strontium carbonate via postdeposition absorption of atmospheric CO_2 through the

dx.doi.org/10.1021/ic201751q | *Inorg. Chem.* 2011, 50, 12396–12398

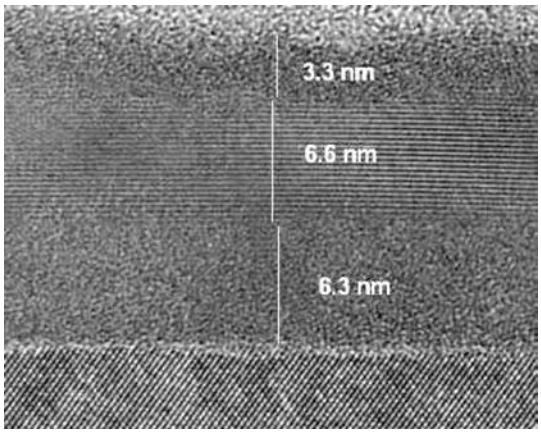

Figure 3. Transmission electron microscopy image of SrO grown at 375 °C from precursor **3** using ozone as oxidant.

thin titanium oxide film. No strontium carbonate was detected by XRD within the SrO film.

In summary, we have opened a new chapter in precursor chemistry by developing volatile strontium and barium imidazolate complexes of exceptional thermal stability, clean volatility, and low melting points. A detailed study of the ALD processes for SrO, BaO, STO, and BST utilizing these unique precursors is in progress and will be reported in a full paper.

■ ASSOCIATED CONTENT

Supporting Information

Synthesis of imidazoles and their strontium and barium complexes, modeling conditions, ALD, GCMS, and CIF files for **1**−**4**, and $^{t}Bu_3$imidazole. This material is available free of charge via the Internet at http://pubs.acs.org.

■ AUTHOR INFORMATION

Corresponding Author

*E-mail: normanja@airproducts.com.

■ REFERENCES

(1) Lee, S. W.; Han, J. H.; Han, S.; Lee, W.; Jang, J. H.; Seo, M.; Kim, S. K.; Dussarrat, C.; Gatineau, J.; Min, Y.; Hwang, C. S. *Chem. Mater.* **2011**, *23*, 2227−2236.

(2) (a) Kosola, A.; Putkonen, M.; Johansson, L.; Niinisto, L. *Appl. Surf. Sci.* **2003**, *211*, 102−112. (b) Kwong, O. S.; Kim, S. K.; Cho, M.; Hwang, C. S.; Jeong, J. *J. Electrochem. Soc.* **2005**, *152* (4), C229−C236.

(3) Hatanpaa, T.; Ritala, M.; Leskela, M. *J. Organomet. Chem.* **2007**, *692*, 5256−5262.

(4) Holme, T. P.; Prinz, F. B. *J. Phys. Chem. A* **2007**, *111*, 8147−8151.

(5) (a) Popovici, M.; Van Elshocht, S.; Menou, N.; Swerts, J.; Pierreuz, D.; Delabie, A.; Britjs, B.; Conard, T.; Opsomer, K.; Maes, J. W.; Wouters, D. J.; Kittl, J. A. *J. Electrochem. Soc.* **2010**, *157* (1), G1−G6. (b) Vehkamaki, M.; Hatanpaa, T.; Ritala, M.; Leskela, M.; Vayrynen, S.; Rauhala, E. *Chem. Vap. Deposition* **2007**, *13*, 239−246.

(6) Schumann, H.; Gottfriedsen, J.; Demtschuk, J. *Chem. Commun.* **1999**, 2091−2092.

(7) Perera, J. R.; Heeg, M. J.; Winter, C. H. *Organometallics* **2000**, *19*, 5263−5265.

(8) Blanco, F.; Alkorta, I.; Elguero, J. *J. Phys. Org. Chem.* **2009**, *22*, 747−755.

(9) (a) Hitzbleck, J.; Deacon, G. B.; Ruhlandt-Senge, K. *Angew. Chem., Int. Ed.* **2004**, *43*, 5218−5220. (b) El-Kaderi, H. M.; Heeg, M. J.; Winter, C. H. *Polyhedron* **2005**, *24*, 645−653. (c) Hitzbleck, J.; O'Brian, A. Y.; Deacon, G. B.; Ruhlandt-Senge, K. *Inorg. Chem.* **2006**, *45*, 10329−10337.

(10) (a) Hitzbleck, J.; O'Brian, A. Y.; Forsyth, C. M.; Deacon, G. B.; Ruhlandt-Senge, K. *Chem.—Eur. J.* **2004**, *10*, 3315−3323. (b) O'Brian, A. Y.; Hitzbleck, J.; Torvisco, A.; Deacon, G. B.; Ruhlandt-Senge, K. *Eur. J. Inorg. Chem.* **2008**, 172−182.

(11) Price, D. M. *Thermochim. Acta* **2001**, *367*−*368*, 253−262.

(12) (a) Delley, B. *J. Chem. Phys.* **1990**, *92*, 508. (b) Delley, B. *J. Chem. Phys.* **2000**, *113*, 7756.

(13) (a) Aihara, J.; Yoshida, M. *J. Mol. Graphics Modell.* **2001**, *19*, 194−198. (b) Aihara, J. *J. Phys. Chem. A* **1999**, *103*, 7487−7495.